LAWRENCE
LIVERMORE
NATIONAL
LABORATORY

LLNL-JRNL-693607

Effect of Equilibration Time on Pu Desorption from Goethite

J. Wong, M. Zavarin, J. Begg, A. B. Kersting, B. A. Powell

June 1, 2016

Radiochimica Acta

Disclaimer

Effect of Equilibration Time on Pu Desorption from Goethite

Jennifer C. Wong,*,† Mavrik Zavarin,‡ James D. C. Begg,‡ Annie B. Kersting,‡ Brian A. Powell*,†

†Department of Environmental Engineering and Earth Sciences, Clemson University, 342 Computer Court, Anderson, South Carolina 29625, USA

‡Glenn T. Seaborg Institute, Lawrence Livermore National Laboratory, 7000 East Avenue, Livermore, California 94551, USA

*Corresponding authors: Brian A. Powell, 342 Computer Court, Anderson, SC 29625, USA, bpowell@clemson.edu; Jennifer C. Wong, jwong@clemson.edu.

Received; accepted

It has been suggested that strongly sorbing ions such as plutonium may become irreversibly bound to mineral surfaces over time which has implications for near- and far-field transport of Pu. Batch adsorption–desorption data were collected as a function of time and pH to study the surface stability of Pu on goethite. Pu(IV) was adsorbed to goethite over the pH range 4.2 to 6.6 for different periods of time (1, 6, 15, 34 and 116 days). Following adsorption, Pu was leached from the mineral surface with desferrioxamine B (DFOB), a complexant capable of effectively competing with the goethite surface for Pu. The amount of Pu desorbed from the goethite was found to vary as a function of the adsorption equilibration time, with less Pu removed from the goethite following longer adsorption periods. This effect was most pronounced at low pH. Logarithmic desorption distribution ratios for each adsorption equilibration time were fit to a pH-dependent model. Model slopes decreased between 1 and 116 days' adsorption time, indicating that overall Pu(IV) surface stability on goethite surfaces becomes less dependent on pH with greater adsorption equilibration time. The combination of adsorption and desorption kinetic data suggest that non-redox aging processes affect Pu sorption behavior on goethite.

Introduction

The production and testing of nuclear weapons have resulted in a legacy of plutonium (Pu) contamination in the environment [1–4]. The mobility of Pu in the subsurface is of particular concern due to the long half-life of Pu (24,000 years for ^{239}Pu) and its radiotoxicity. Pu sorption to minerals is the main mechanism controlling its subsurface mobility. Sorption of Pu to iron oxides, of which goethite (α–FeOOH) is one of the most common, is of key interest because iron oxides are ubiquitous in the environment [5, 6]

and Pu exhibits a very high affinity for iron oxide surfaces. Although it is generally assumed that that Pu is relatively immobile due to its low solubility [7–10] and strong sorption of Pu(IV) to mineral surfaces [11], long-distance transport of Pu has been observed in association with colloids [12–14], suggesting formation of highly stable Pu surface complexes on colloids. At the Mayak site, colloid-facilitated transport appeared to be driven by Pu association with iron oxide colloids [13], In sorption experiments with soluble Pu(V) and goethite colloids in natural groundwater, it was concluded that Pu desorption rates are much slower than adsorption rates [15, 16]. In acid leaching experiments, stabilization of sorbed nanocrystalline Pu on hematite was observed with increasing contact time [17]. Thus it is hypothesized that observations of colloid-facilitated transport are due to irreversible sorption or rate-limited desorption of Pu to colloids or rate-limited desorption of Pu from colloids [18, 19]. This hypothesis is supported by field studies in which long distance, colloid-facilitated transport of Pu has been observed [12, 13, 20].

An irreversible reaction is an “exothermic reaction in which the activation energy for the reverse reaction is sufficiently large that the reaction proceeds only in the forward direction under practical conditions” [21]. When used in the context of sorption reactions, irreversibility is characterized by an inequality between adsorption and desorption distribution coefficients. However, sorption reactions which appear irreversible on short timescales (hours to days) may actually be reversible and simply have very slow rates of adsorption or desorption. In this case, as adsorption or desorption times are increased beyond typical laboratory timescales, the inequality between adsorption and desorption distribution coefficients may vanish.

Aging is a “surface chemical process that follows the initial sorption reaction and causes changes in contaminant surface speciation over time” [22]. These changes in surface speciation could make the contaminant more stable on the surface. Aging is manifested by distribution coefficients which increase with contact time. As a result, the amount of contaminant which can be desorbed decreases with increasing contact time. Depending on the timescales of adsorption/desorption, aging can give the appearance of irreversible sorption. Thus, the irreversible adsorption attributed to colloid facilitated Pu transport at the Mayak Site [13] and the slow desorption rates observed in batch Pu goethite sorption experiments [15, 16] could be attributed to aging.

Though several hypotheses regarding the underlying mechanisms of aging (or irreversible sorption) have been proposed, few have been explicitly proven. The sorbate may undergo a change in surface speciation over time, either by the formation of shorter and stronger bonds with the surface or by the physical transfer of the sorbate to sites of higher reactivity [23–26]. As goethite is a microporous mineral [27, 28], aging on goethite may also occur by aqueous diffusion into micropores followed by sorption to interior sites [17, 23–26, 29–32]. Surface precipitation of the sorbate has been suggested as an aging process [24, 25, 31]. Another proposed aging process is surface exchange,

where a sorbate atom exchanges with an iron atom in the mineral lattice and becomes structurally incorporated [33]. Incorporation of the sorbate as a result of mineral recrystallization has also been identified as an aging process [26, 31, 32, 34]. Surface mediated reduction of Pu(V) to Pu(IV), which has been observed on iron oxide and other mineral surfaces [35–39] may also exhibit the characteristics of an aging process. In cases where researchers have observed a rapid sorption step followed by a second, slow sorption step, the second reaction has been attributed to diffusion of Pu into micropores or surface mediated reduction of Pu(V) [35, 40].

Regardless of the proposed aging mechanisms discussed above, numerical descriptions of aging are typically parameterized as two consecutive reactions: an initial sorption reaction followed by a second aging reaction. This consideration of multiple kinetic sites is necessary to evaluate aging processes. Since sorption of ions to the initial sites appears to be rapid, the rate of the second reaction should be the rate limiting step. Thus, the rate of slow uptake commonly observed in the second phase of a kinetic sorption experiment could be a proxy of the aging process on the surface.

Pu Redox Behavior and Sorption on Iron Oxides

Plutonium can exist in the +III, +IV, +V and +VI valence states simultaneously under natural conditions [41, 42]. At moderate pH and E_h, Pu(IV) and Pu(V) are the dominant oxidation states, whereas Pu(III) and Pu(VI) are generally only stable under anoxic or oxic conditions, respectively [43]. Due to the profound insolubility of Pu(IV), it is commonly found in ligand-free solutions as a precipitate or sorbed to solid phases. Conversely, Pu(V) is more soluble and the stable oxidation state of aqueous Pu in dilute salt solutions and seawater [44, 45]. Therefore, a common observation is that Pu(V) is the dominant aqueous phase oxidation state and Pu(IV) is the dominant oxidation state in solid phases. This is illustrated by the solubility of $PuO_{2(s)}$ phases under oxic conditions where the solubility limit is approximately 10^{-8} to 10^{-6} M with the aqueous phase dominated by Pu(V) [7, 46–48].

The distribution of Pu(IV) and Pu(V) oxidation states primarily between solid and aqueous, phases, respectively, has also been observed in sorption experiments [35, 36, 38–40, 49–51]. The sorption edges of Pu(IV) and Pu(V) correlate with the hydrolysis of Pu in these oxidation states [7–10, 35, 36]. On goethite, the sorption edge for Pu(IV), which begins to hydrolyze [7–10, 52] to $Pu(OH)_x^{4-x}$ species at pH 1, is in the pH range 3 to 5 [35, 52]. After 24 hours, the sorption edge for Pu(V) is in the pH range 6 to 8, which is consistent with the expected hydrolysis of Pu(V) at pH <9.7 [35, 52]. However, Pu(V) undergoes surface mediated reduction to Pu(IV) on iron oxides, leading to a shift in the sorption edge to a lower pH over time [35–39]. Thus, if Pu(V) is present in the pH range 3 to 8 the fraction of sorbed Pu is observed to increase over time [35–39]. The dominance of aqueous Pu(V) and its reduction implies that

reduction of Pu(V) to Pu(IV) is a surface mediated process. Few desorption studies have been performed which monitor the aqueous oxidation state of desorbed Pu. Thus, it is unclear if desorption is coupled with a surface mediated oxidation step. Using $PuO_{2(s)}$ solubility studies as a proxy for desorption studies, similar dominance of aqueous Pu(V) has been observed [46–48].

Because multiple Pu oxidation states may be present simultaneously, it is necessary to know the distribution of sorbed and aqueous oxidation states in sorption experiments [53]. One method to simplify the system is to add an organic ligand which can stabilize aqueous Pu(IV) and avoid the formation of Pu(V). In this case, the amount of Pu which can be desorbed from the mineral surface can be related to the relative stability of the Pu(IV)–surface and the Pu(IV)–ligand complexes without needing to address the additional complexity of Pu(IV) oxidation.

Desferrioxamine B (DFOB) can be used to stabilize Pu(IV) as the dominant aqueous oxidation state across a wide range of experimental conditions (pH, concentration, atmospheric conditions; Fig. A1) [54, 55]. In addition, the aqueous Pu(IV)–DFOB complex can effectively promote Pu(IV) desorption from goethite. Equilibrium speciation calculations under atmospheric conditions show that Pu(IV)–DFOB complexes dominate over $Pu(OH)_x^{4-x}$ species between pH 4 and 8 at concentrations of 10^{-10} M Pu(IV) and 1.7 µM DFOB (Fig. A2). Under these conditions, the high stability of Pu(IV)–DFOB complexes are expected to thermodynamically maintain the dominance of the aqueous Pu(IV)–DFOB complexes and minimize Pu(IV) oxidation to Pu(V) under atmospheric conditions (Fig. A1).

In this work, an alternative approach to examining aging has been utilized wherein desorption of Pu is monitored using a strong aqueous complexant (i.e. DFOB) that promotes Pu desorption and controls the Pu oxidation state. Adsorption equilibration periods as long as 4 months were examined to test the existence of very slow aging processes. Desorption was carried out after a 34 day equilibration period for the same reasons. The overall surface stability of Pu as a function of adsorption equilibration time was quantified by examining the linear relationship between logarithmic distributions ratios ($log\ R_d$) and pH values.

Materials and Methods

Acids and bases used were Aristar Plus grade. Cyclohexane (Alpha Aesar) and sodium chloride used were ACS reagent grade. All water used was distilled and deionized with resistivity >18 MΩ·cm. A DFOB stock solution was prepared at a concentration of 1.7 mM by dissolving desferoxamine mesylate salt (Sigma Aldrich) in deionized water.

The goethite was prepared as described previously [22] and had a BET surface area of 42 m^2/g. A goethite stock suspension of 8.0 g/L was prepared by suspending goethite in 100 mL deionized water, centrifuging to a particle size cutoff of 100 nm, and replacing supernatant with fresh

deionized water. This washing step was performed three times to remove <100 nm goethite fines. The final goethite stock was suspended in 100 mL 10 mM NaCl.

Concentrations of ^{238}Pu were measured by liquid scintillation counting. Samples were prepared for alpha spectroscopic analysis with Optiphase Hisafe 3 scintillation cocktail (Perkin Elmer) and counted with alpha/beta discrimination using a Wallac model 1415, Hidex 300SL, or Perkin Elmer Tri-Carb 2910 TR liquid scintillation counter. For each instrument, Pu stock solutions were measured so that aqueous Pu concentrations could be calculated as a fraction of Pu added to samples.

Concentrations of ^{238}Pu were measured by liquid scintillation counting. Samples were prepared for alpha spectroscopic analysis with Optiphase Hisafe 3 scintillation cocktail (Perkin Elmer) and counted with alpha/beta discrimination using a Wallac model 1415, Hidex 300SL, or Perkin Elmer Tri-Carb 2910 TR liquid scintillation counter. For each instrument, Pu stock solutions were measured so that aqueous Pu concentrations could be calculated as a fraction of Pu added to samples.

Pu Stock Solutions and Oxidation State Analyis

A stock solution of 6.6×10^{-8} M ^{238}Pu(IV) was prepared by evaporating ^{238}Pu(V) stock (Isotope Products) in 1 M HNO_3 and redissolving in 0.1 M HCl. A Pu–DFOB stock solution was prepared by adding DFOB to 1 mL Pu(IV) stock solution to yield 3.3×10^{-5} M DFOB and 5.9×10^{-8} M Pu. Because the Pu concentrations in stock solutions and samples were too low to use direct observation techniques (e.g. UV-Vis spectroscopy), well-established co-precipitation and solvent extraction techniques were used to determine Pu oxidation state. The oxidation state of the DFOB-free Pu(IV) stock solution was verified to be 91.9 ± 0.6 % Pu(IV) by lanthanum fluoride co-precipitation [56, 57]. The oxidation state of some DFOB-free samples was measured by organic solvent extraction with 0.025 M 1-phenyl-3-methyl-4-benzoyl-pyrazole-5-one (PMBP; Tokyo Chemistry Industry Co., Ltd.) in cyclohexane, which extracts Pu(IV) into the organic phase, leaving oxidized Pu in the aqueous phase [10, 58]. Aqueous and organic fractions of Pu were measured by liquid scintillation counting with alpha/beta discrimination. The Pu oxidation state of the solutions containing DFOB could not be verified due to interference of DFOB with the co-precipitation reaction and solvent extraction. The oxidation state of Pu in the Pu–DFOB stock solution is assumed to be Pu(IV) based on the initial Pu(IV) state of the stock solution and the strong complexation of DFOB with Pu(IV) [54].

Pu Batch Adsorption–Desorption in the Presence and Absence of DFOB

An adsorption–desorption batch experiment with Pu was performed on goethite suspensions as a function of pH to establish that the presence of DFOB will limit Pu

adsorption and enhance Pu desorption compared to a DFOB-free solution. Solutions of 10 mM NaCl and 0.075 g/L goethite were prepared in 15 mL polyethylene tubes. After addition of Pu from Pu(IV) or Pu–DFOB stock solutions, the final Pu concentration of samples was $\approx 1.7 \times 10^{-10}$ M for DFOB-containing samples and $\approx 1.9 \times 10^{-10}$ M for DFOB-free samples. The total Pu added to each sample from stock solutions was determined gravimetrically. Additional DFOB was added to DFOB-containing samples from the DFOB stock solution to yield 1.7 µM DFOB. Sample pH values were adjusted to 6 and 8 with dilute HCl and NaOH. During adsorption, aqueous Pu was measured at 2 hours, 5 hours, 1, 3, 10, and 25 days. Then, the supernatant was replaced with either 1.7 µM DFOB or DFOB-free solution, and aqueous Pu was monitored during desorption (see Supporting Information). Sampling consisted of transferring a 1.4 mL homogenous aliquot to a microcentrifuge tube, centrifugation at 8000 rpm for 20 minutes (Beckman and Coulter Allegra 22R centrifuge with F2402 rotor) which is calculated to remove particles >100 nm based on Stoke's Law, and measuring the Pu concentration in the supernatant. First-order adsorption rate constants were estimated by fitting measurements spanning 2 hours – 25 days.

Effect of Adsorption Equilibrium Time on Pu(IV) Surface Stability

Preliminary experiments suggested that Pu(IV) desorption behavior was dependent on adsorption time. To test the effect of adsorption time on desorption behavior, DFOB-free solutions of 10 mM NaCl and 0.10 g/L goethite were prepared in 1.5 mL microcentrifuge tubes in duplicate. The Pu(IV) stock solution was spiked into each sample to yield $\approx 1.2 \times 10^{-10}$ M Pu. The total Pu added to each sample from stock solutions was determined gravimetrically. The samples were initially adjusted to pH 4, 5, 6, 7 and 8 using dilute HCl and NaOH, but allowed to drift during the adsorption period. Most of the pH drift occurred in the first day. The final pH range spanned 4.2 to 6.6.

Samples were allowed to equilibrate for 1, 6, 15, 34 and 116 days. Following the adsorption step, samples were centrifuged to remove particles >100 nm from the supernatant and the Pu concentration in the supernatant was measured. Then, the supernatant was quantitatively replaced with a 1.7 µM DFOB solution adjusted to pH 4, 5, 6, 7, and 8 using dilute HCl and NaOH. Desorption of Pu from each sample was allowed to occur for 34 days for all samples, regardless of the initial equilibration time. Finally, samples were centrifuged to remove particles >100 nm from the supernatant and the Pu concentration in the supernatant was measured.

Use of DFOB in Pu–Goethite Sorption Experiments

DFOB was used to enhance desorption of Pu and to stabilize Pu(IV) as the dominant aqueous oxidation state. Although DFOB strongly complexes Fe(III) in aqueous

solution, DFOB has been shown to interact weakly with the goethite surface at pH 3 to 9 due to electrostatic repulsion of the cationic DFOB and also to steric hindrance [59–61]. Based on previous DFOB–goethite sorption isotherms [59, 60] at pH 5 and 6.6, it is estimated that for 1.7 µM total DFOB and 0.1 g/L goethite only 2–6 % of DFOB sorbs (see Appendix). Furthermore, despite the formation of strong Fe(III)–DFOB complexes, low dissolution rates of 0.01 to 0.02 µmol/(g·h) are observed for goethite in the presence of DFOB [60, 62]. Therefore, as will be discussed below, Pu–ligand complexation rather than goethite dissolution is the driving mechanism for release of sorbed Pu. The dissolution of goethite was tested by measuring aqueous iron concentrations in the presence of DFOB by Inductively Coupled Plasma Mass Spectrometry, (ICP-MS, Thermo Scientific XSeries 2).

Because DFOB interacts weakly with goethite surfaces, formation of ternary goethite–DFOB–Pu surface complexes is expected to be minimal. As a result, DFOB is expected to have little effect on Pu surface speciation and only facilitate desorption of Pu. For the experimental conditions of this work, our conceptual model is that Pu sorption to goethite may be treated as a binary system of ≡FeOH–Pu(IV) surface complexes and aqueous Pu(IV)–DFOB complexes. Thus, differences in measured distribution ratios can be attributed directly to changes in the binding energy of the ≡FeOH–Pu(IV) surface complex.

Calculations

All data are presented as percent sorbed, percent desorbed, or a distribution ratio. Distribution ratios, R_d (mL/g), were calculated from the aqueous Pu concentration, $C_{Pu,aq}$ (mol/L), and the total Pu added to each sample, $C_{Pu,total}$ (mol/L), according to Equation 1, where SS (g/L) represents the suspended solids concentration

$$R_d = \frac{C_{Pu,total} - C_{Pu,aq}}{C_{Pu,aq}} \cdot \frac{1000}{SS} \quad (1)$$

Distribution ratios are not equivalent to the more traditional distribution coefficient, K_d, because in the former case, an equilibrium condition is not assumed. For adsorption measurements, the percent sorbed was calculated based on the total Pu added at the beginning of the experiment. For desorption measurements, the percent (de)sorbed was calculated based on the estimated total Pu remaining in samples after the supernatant was exchanged.

Least-squares regression fitting was used to estimate the first-order adsorption rate constants, k_f (s^{-1}), according to Equation 2, where t is adsorption time in seconds. During fitting, the aqueous Pu concentration at time zero, $C_{Pu,aq}(0)$, and k_f were treated as adjustable parameters.

$$C_{Pu,aq}(t) = C_{Pu,aq}(0)e^{-k_f t} \quad (2)$$

Results and Discussion

Pu Batch Adsorption–Desorption in the Presence and Absence of DFOB

In all samples, there is a rapid Pu adsorption step that occurs within the first 2 hours (Fig. 1). After 2 hours, the extent of Pu sorption tends to increase slowly for at least 25 days in DFOB and DFOB-free solutions. Thus, it appears that adsorption aging effects exist both in the presence and absence of DFOB.

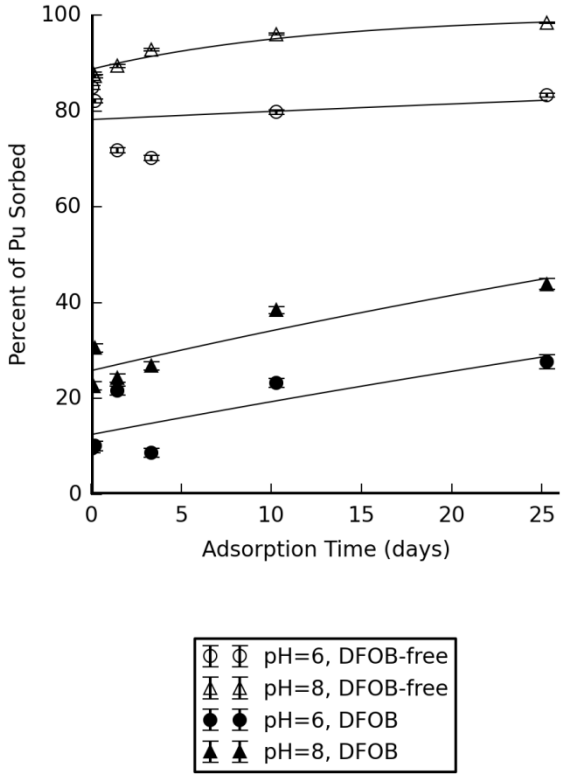

Fig. 1. Adsorption of Pu on a 0.075 g/L goethite suspension with 10 mM NaCl for ionic strength control. Pu was initially added as Pu(IV). Solutions contained 1.7 µM DFOB or were DFOB-free. Lines indicate first-order rate models fit to the data. Error bars represent two standard deviations of measurement uncertainty derived from counting statistics. The first data point was collected after a 2 hour adsorption time period.

Between 2 hours and 25 days, the percent Pu sorbed in DFOB-containing samples increases from 9.7 ± 0.5 % to 27.7 ± 0.8 % and from 22.6 ± 0.4 % to 43.9 ± 0.6 % at pH 6 and 8, respectively. As a result of DFOB stabilizing Pu(IV) in solution, surface mediated reduction of Pu(V) should not be a relevant aging mechanism in these samples. Thus, we attribute the increase in sorption to non-redox aging effects.

The percent Pu sorbed for the DFOB-free sample increases between 2 hours and 25 days from 87.74 ± 0.16 % to 98.40 ± 0.07 % at pH 8. It is noteworthy that in the absence of DFOB, Pu(IV)/Pu(V) redox transformations may influence the partitioning of Pu. Oxidation state analysis of aqueous Pu in DFOB-free samples with solvent extraction confirms

that Pu(V/VI) is the stable aqueous form of Pu in these samples. In samples adsorbed for 25 days at pH 6 and 8, 97 ± 7 % and 100 ± 12 % of supernatant Pu is in the V/VI oxidation state, respectively. However, the surface area normalized adsorption rate observed at pH 8 ($1.08 \pm 0.10 \times 10^{-3}$ L/(m^2·h)) is much lower the published rate of surface mediated reduction of Pu(V) ($2.3 \pm 0.7 \times 10^{-2}$ L/(m^2·h)) [38]. Thus, despite the likely occurrence of redox transformations at early time (days), some process other than surface mediated reduction of Pu(V) is responsible for observed aging behavior in the presence and absence of DFOB over the long term.

The presence of DFOB causes a marked decrease in the percent of sorbed Pu (Fig. 1), and greater sorption is observed at pH 8 relative to pH 6. Aqueous equilibrium speciation modeling indicates Pu speciation in 1.7 μM DFOB at pH 6 and 8 under atmospheric conditions is dominated by $PuH_2(DFOB)_2^{2+}$ rather than $Pu(OH)_x^{4-x}$ species (Figs. A1 and A2). Because ternary goethite–DFOB–Pu complexes are not expected to form, the slightly greater sorption at pH 8 relative to pH 6 is likely due to the increased stability of Pu(IV)–goethite surface complexes with increasing pH.

Dissolved iron measurements in the presence of DFOB were below the ICP-MS detection limit of 2.8 μM. However, given that the DFOB concentration is only 1.7 μM, competition between Fe and Pu for DFOB may have occurred in these samples. Nevertheless, the enhanced aqueous concentration of Pu in the presence of DFOB indicates that the Pu–DFOB complexes can form despite a portion of DFOB forming Fe–DFOB complexes. Some Pu desorption as a result of goethite dissolution may have occurred. However, the amount of goethite surface area available for Pu sorption did not decrease over the course of these experiments. Thus, we can conclude that formation of soluble Pu-DFOB complexes is the dominant mechanism responsible for the higher aqueous Pu concentrations in the presence of DFOB.

After 25 days' adsorption, the samples were phase separated and supernatants exchanged for fresh Pu-free solutions of the same pH and DFOB concentration as in the initial adsorption step. In less than 3 hours, desorption was greater in DFOB samples than DFOB-free samples (Fig. A4). At 3 hours, the percent of Pu remaining sorbed in DFOB solutions was 74.8 ± 0.4 % and 85.2 ± 0.30 % at pH 6 and 8, respectively. In contrast, the percent of Pu remaining sorbed in DFOB-free solutions was 96.44 ± 0.11 % and 97.3 ± 0.09 % at pH 6 and 8, respectively. Importantly, in the presence of DFOB, Pu desorption experiments appear to have reached equilibrium after 18 hours. In the DFOB-free samples, the pH 8 Pu desorption experiment neared equilibrium by three days while the pH 6 experiment approached equilibrium much more slowly. Thus, it is apparent that DFOB can effectively facilitate and accelerate Pu desorption from goethite and that desorption equilibrium is achieved on the timescale of days.

Results of Varying Adsorption Equilibrium Time

In order to test the effect of adsorption equilibration time (in the absence of DFOB) on Pu surface stability, a batch adsorption–desorption experiment was conducted on goethite suspensions with varying adsorption times in DFOB-free solution and a constant desorption time of 34 days in 1.7 μM DFOB solution. The DFOB-free adsorption data (Fig. 2) support the conceptual model of Pu aging on the goethite surface. This aging is seen as a steady shift in the sorption edge towards lower pH values for up to 116 days. This is in contrast to previously observed rates of surface mediated reduction, where greater than 90% of Pu(V) reduction was observed within 24 hours [38]. Thus, the observed aging is likely the result of a mechanism other than surface mediated reduction occurring on the goethite surface.

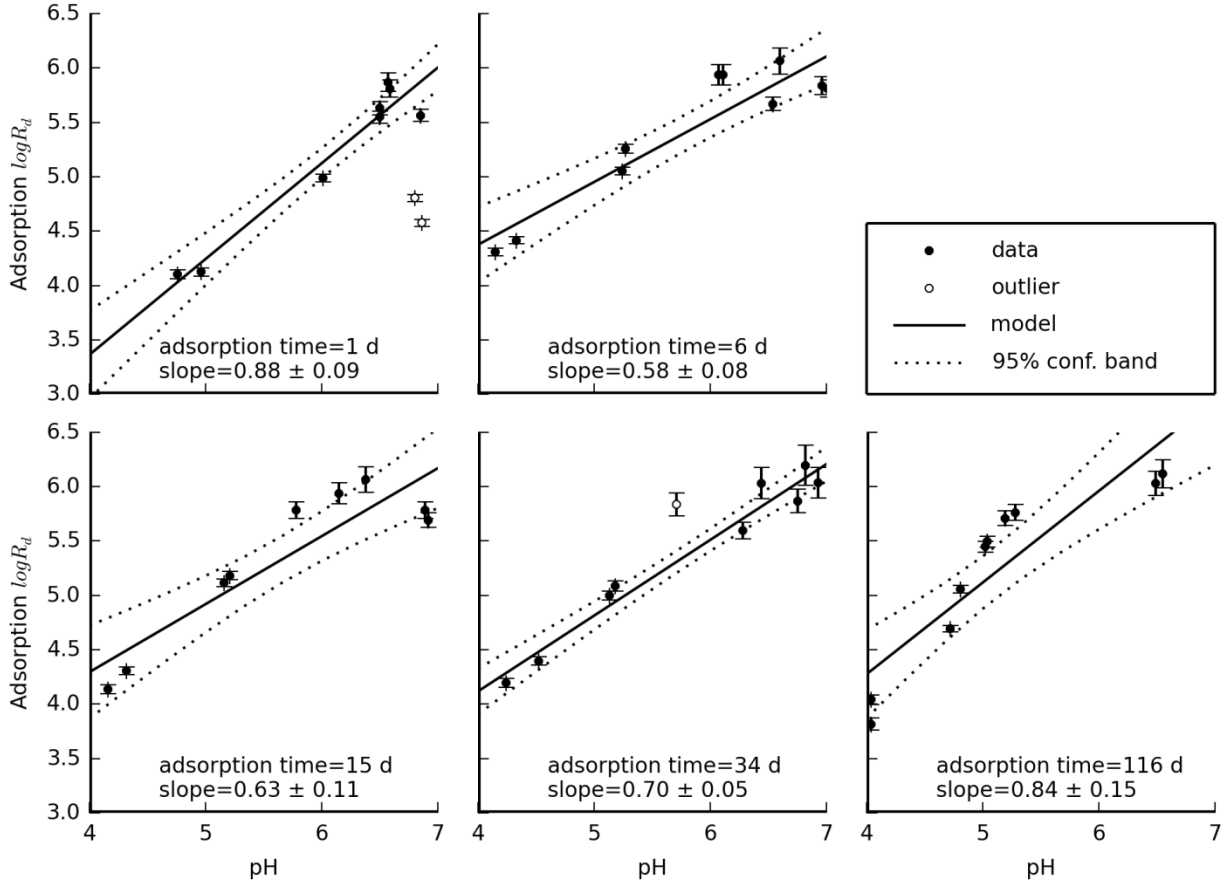

Fig. 2. Logarithmic adsorption distribution ratios (R_d) for Pu on 0.10 g/L goethite suspensions as a function of pH and time. Total Pu concentration is 1.2×10^{-10} M, and ionic strength was controlled with 10 mM NaCl. Error bars indicate two standard deviations of measurement uncertainty derived from counting statistics.

The effect of aging on Pu desorption was tested by performing a 34 day desorption in 1.7 μM DFOB solution on each of the adsorption samples. The 34 days provided

ample time for samples to reach equilibrium (Fig. A4). The decrease in percent DFOB-desorbable Pu with increasing adsorption time is indicative of Pu stabilization on the goethite surface (Fig. 3). During DFOB-free adsorption at pH 4, we can expect only trace amounts of Pu(V) to be sorbed to the goethite surface [35]. Thus, aging behavior at pH 4 must be the result of Pu(IV) stabilization on the goethite surface and not Pu(IV)/(V) redox transformations.

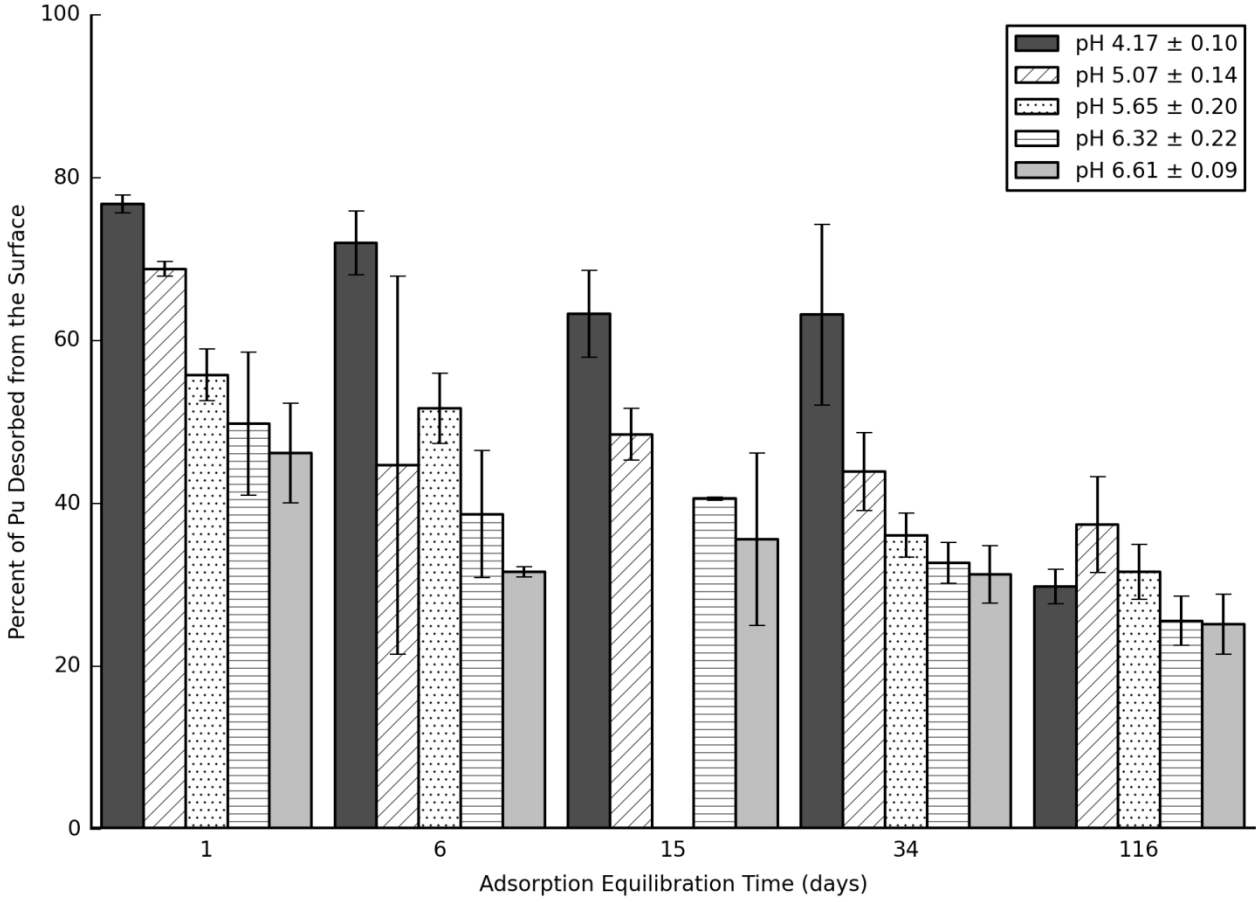

Fig. 3. The percent of Pu desorbed is plotted against adsorption equilibration time. Samples initially contained 1.2×10^{-10} M total Pu before supernatant replacement and desorption with 1.7 µM DFOB for 34 days. The mean pH values of each sample group are shown in the legend. Goethite suspension concentration was 0.10 g/L, and ionic strength was controlled with 10 mM NaCl. Error bars indicate the standard deviation of duplicates.

The aging behavior observed in the desorption data is more pronounced at lower pH values. At pH 4.2, the percent Pu desorbed decreases from 76.8 ± 1.1 % to 29.8 ± 2.1 % between 1 and 116 days of adsorption equilibration, and, at pH 6.6, the percent of Pu desorbed decreases from 46 ± 6 % to 25 ± 4 %, for the same periods of adsorption. The greater change over time in the percent Pu desorbed suggests that aging is pH-dependent. The pH-dependence may reflect the presence of a strongly sorbing (and less labile) form of Pu on the goethite surface at high pH values. However, the underlying reason for the pH dependence cannot be identified with these data.

To further evaluate the pH- and time-dependence of desorption, logarithmic desorption R_d values for each adsorption equilibration time were plotted against pH (Fig. 4) and were fit with a linear model which considers a pH-dependent and a pH-independent term (Eq. 3).

$$logR_d = slope \times pH + intercept \quad (3)$$

For samples adsorbed for 1 to 34 days, the estimated slopes range from 0.2 to 0.32, while at 116 days, the slope decreases to 0.06. These results suggest that Pu surface stability becomes less pH-dependent with increasing adsorption equilibration time. It also suggests that a pH-independent R_d value may describe the Pu desorption from goethite at longer, environmentally relevant timescales.

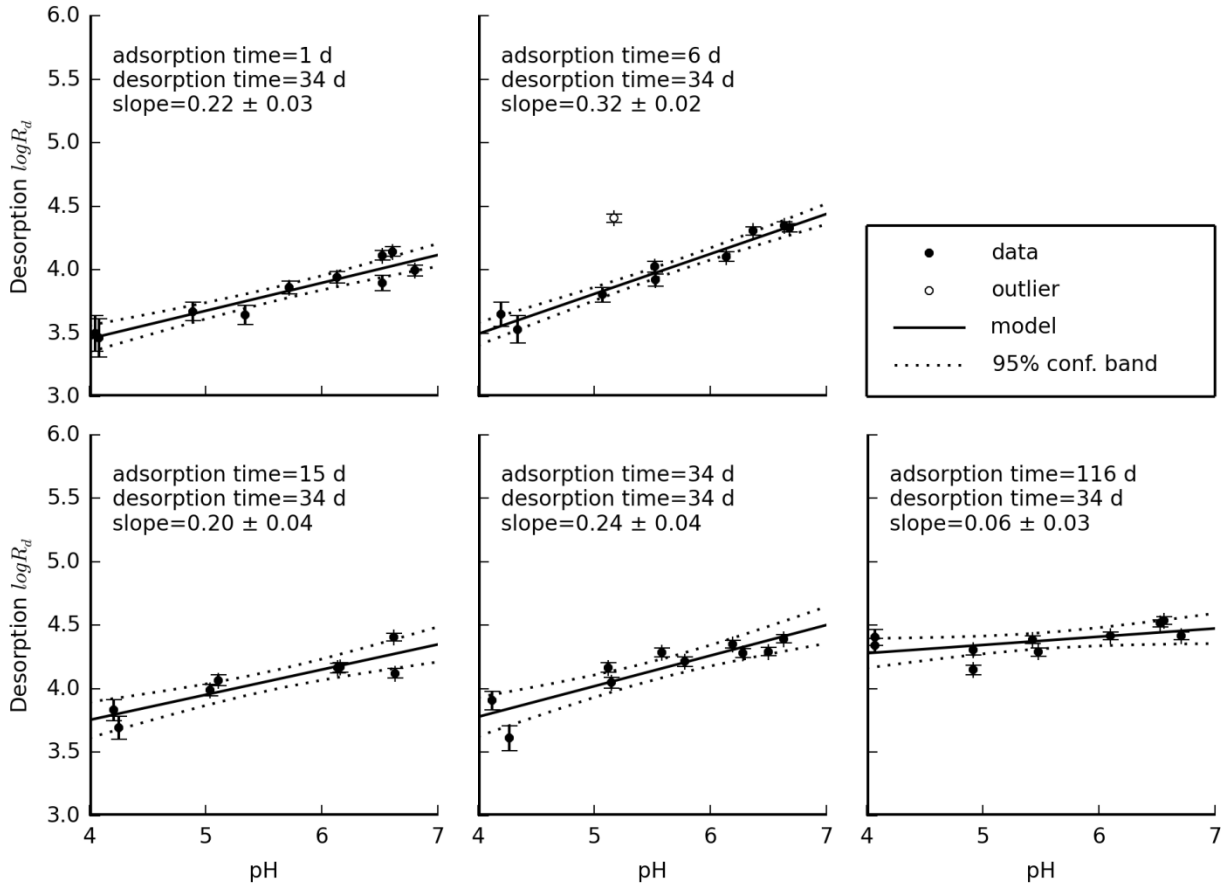

Fig. 4. Logarithmic desorption distribution ratios (R_d) for Pu resulting from adsorption in DFOB-free solution for various equilibration times (indicated), supernatant replacement, and desorption in 1.7 µM DFOB solution for 34 days. Total Pu was originally 1.2×10^{-10} M before supernatant replacement. Goethite suspension concentration was 0.10 g/L, and ionic strength was controlled with 10 mM NaCl. Error bars indicate two standard deviations of measurement uncertainty derived from counting statistics. Shown are linear models which consider a pH-dependent and a pH-independent term.

The pH-dependent aging and time-dependent desorption behavior in the presence and absence of DFOB can be used to identify the aging processes that may play a role in Pu sorption behavior. Pu adsorption data in the presence of

DFOB suggest that a non-redox, aging mechanism plays a role in stabilizing Pu(IV) on the goethite surface. In the absence of DFOB, the pH- and time-dependent adsorption rates are slower than previously reported rates of surface mediated Pu(V) reduction on goethite. The initial Pu(IV) stock solution contained ≈10% Pu(V). Thus, while redox transformations likely played a role in Pu adsorption rates at early times (days), the observed aging on a timescale of weeks is not consistent with surface mediated reduction processes. The decrease in Pu desorption as a function of equilibration time, particularly at pH 4, provides clear evidence that Pu(IV) sorbed to goethite becomes more stable with time. At higher pH values, the effect is less pronounced, suggesting a pH-dependence to this aging process.

Implications of Aging on Pu Subsurface Migration

The aging phenomena observed in this work may impact the fate and transport of Pu in the environment. As natural soils contaminated with Pu age, the strength of Pu sorption to bulk soil will increase with increasing time and make Pu less labile. Importantly, the aging process has been shown to include non-redox mechanisms. Furthermore, R_d values based on short term adsorption or desorption experiments will underestimate long term equilibrium K_d values, and lead to overestimated *aqueous* Pu transport distances. Conversely, if Pu is sorbed to mobile colloids, aging may result in formation of stronger Pu–colloid associations and, thus, lead to greater colloid-facilitated Pu transport distances. These aging phenomena support the frequent observations of colloid-facilitated Pu transport [12, 13] wherein Pu can be transported significant distances adsorbed to the colloid on a timescale of years. Furthermore, the pH dependency of aging implies that the magnitude of this effect will be dependent on the local geochemical conditions but will occur regardless of whether Pu redox transformation is prevalent.

Acknowledgements. This work was supported by the Subsurface Biogeochemical Research Program of the U.S. Department of Energy's Office of Biological and Environmental Research. Prepared by LLNL under contract DE-AC52-07NA27344.

References

1. Cantrell, K. J.: Transuranic Contamination in Sediment and Groundwater at the U.S. DOE Hanford Site. Pacific Northwest National Laboratory, Richland, WA. PNNL-18640 (2009).
2. Felmy, A. R.; Cantrell, K. J.; Conradson, S. D.: Plutonium Contamination Issues in Hanford Soils and Sediments: Discharges from the Z-Plant (PFP) Complex. Phys. Chem. Deep Earth **35**, 292–297 (2010) doi:10.1016/j.pce.2010.03.034.
3. Smith, D. K.; Finnegan, D. L.; Bowen, S. M.: An Inventory of Long-Lived Radionuclides Residual from Underground Nuclear Testing at the Nevada Test Site, 1951–1992. J. Environ. Radioact. **67**, 35–51 (2003) doi:10.1016/S0265-931X(02)00146-7.

4. Carlton, W. H.; Evans, A. G.; Geary, L. A.; Murphy, Jr., C. E.; Pinder, J. E.; Strom, R. N.: Assessment of Plutonium in the Savannah River Site Environment. Westinghouse Savannah River Company, LLC, Aiken, SC. WSRC-RP-92-879 Rev.1 (1992).
5. Schwertmann, U.; Taylor, R. M.: Iron Oxides. In: *Minerals in Soil Environments*. Soil Science Society of America, Madison, WI (1989) pp. 379–438.
6. Cornell, R. M.; Schwertmann, U.: *The Iron Oxides: Structure, Properties, Reactions, Occurences and Uses*. 2nd ed. Wiley-VCH, Weinham (2003).
7. Choppin, G. R.: Actinide Speciation in the Environment. Radiochim. Acta **91**, 645–650 (2003) doi:10.1524/ract.91.11.645.23469.
8. Knopp, R.; Neck, V.; Kim, J.: Solubility, Hydrolysis and Colloid Formation of Plutonium (IV). Radiochim. Acta **86**, 101–108 (1999).
9. Neck, V.; Kim, J. I.: Solubility and Hydrolysis of Tetravelent Actinides. Radiochim. Acta **88**, 1–16 (2001).
10. Nitsche, H.; Edelstein, N. M.: Solubilities and Speciation of Selected Transuranium Ions. A Comparison of a Non-Complexing Solution with a Groundwater from the Nevada Tuff Site. Radiochim. Acta **39**, 23–33 (1985).
11. Triay, I. R.; Cotter, C. R.; Kraus, S. M.; Huddleston, M. H.; Chipera, S. J.; Bish, D. L.: Radionuclide Sorption in Yucca Mountain Tuffs with J-13 Well Water: Neptunium, Uranium, and Plutonium. Yucca Mountain Site Characterization Program Milestone 3338. Los Alamos National Laboratory, Los Alamos, NM. LA-12956-MS (1996).
12. Kersting, A. B.; Efurd, D. W.; Finnegan, D. L.; Rokop, D. J.; Smith, D. K.; Thompson, J. L.: Migration of Plutonium in Ground Water at the Nevada Test Site. Nature **397**, 56–59 (1999) doi:10.1038/16231.
13. Novikov, A. P.; Kalmykov, S. N.; Utsunomiya, S.; Ewing, R. C.; Horreard, F.; Merkulov, A.; Clark, S. B.; Tkachev, V. V.; Myasoedov, B. F.: Colloid Transport of Plutonium in the Far-Field of the Mayak Production Association, Russia. Science **314**, 638–641 (2006) doi:10.1126/science.1131307.
14. Santschi, P. H.; Roberts, K. A.; Guo, L.: Organic Nature of Colloidal Actinides Transported in Surface Water Environments. Environ. Sci. Technol. **36**, 3711–3719 (2002) doi:10.1021/es0112588.
15. Lu, N.; Triay, I. R.; Cotter, C. R.; Kitten, H. D.; Bentley, J.: Reversibility of Sorption of Plutonium-239 onto Colloids of Hematite, Goethite, Smectite, and Silica: A Milestone Final Report of YMP. Los Alamos National Laboratory. LA-UR-98-3057 (1998).
16. Lu, N.; Cotter, C. R.; Kitten, H. D.; Bentley, J.; Triay, I. R.: Reversibility of Sorption of Plutonium-239 onto Hematite and Goethite Colloids. Radiochim. Acta **83**, 167–173 (1998).
17. Romanchuk, A. Y.; Kalmykov, S. N.; Egorov, A. V.; Zubavichus, Y. V.; Shiryaev, A. A.; Batuk, O. N.; Conradson, S. D.; Pankratov, D. A.; Presnyakov, I. A.: Formation of Crystalline $PuO_{2+x} \cdot nH_2O$ Nanoparticles upon Sorption of Pu(V,VI) onto Hematite. Geochim. Cosmochim. Ac. **121**, 29–40 (2013) doi:10.1016/j.gca.2013.07.016.
18. Painter, S.; Cvetkovic, V.; Pickett, D.; Turner, D. R.: Significance of Kinetics for Sorption on Inorganic Colloids: Modeling and Experiment Interpretation Issues. Environ. Sci. Technol. **36**, 5369–5375 (2002) doi:10.1021/es025718o.
19. Cvetkovic, V.; Painter, S.; Turner, D.; Pickett, D.; Bertetti, P.: Parameter and Model Sensitivities for Colloid-Facilitated Radionuclide Transport on the Field Scale. Water Resources Research **40**, (2004) doi:10.1029/2004WR003048.
20. Penrose, W. R.; Polzer, W. L.; Essington, E. H.; Nelson, D. M.; Orlandini, K. A.: Mobility of Plutonium and Americium

through a Shallow Aquifer in a Semiarid Region. Environ. Sci. Technol. **24**, 228–234 (1990) doi:10.1021/es00072a012.
21. Fox, M. A.; Whitesell, J. K.: *Organic Chemistry*. Jones and Bartlett Publishers, Sudbury, MAs (2004).
22. Tinnacher, R. M.; Zavarin, M.; Powell, B. A.; Kersting, A. B.: Kinetics of Neptunium(V) Sorption and Desorption on Goethite: An Experimental and Modeling Study. Geochim. Cosmochim. Ac. **75**, 6584–6599 (2011) doi:10.1016/j.gca.2011.08.014.
23. Backes, C. A.; McLaren, R. G.; Rate, A. W.; Swift, R. S.: Kinetics of Cadmium and Cobalt Desorption from Iron and Manganese Oxides. Soil Sci. Soc. Am. J. **59**, 778–785 (1995) doi:10.2136/sssaj1995.03615995005900030021x.
24. Lehmann, R. G.; Harter, R. D.: Assessment of Copper-Soil Bond Strength by Desorption Kinetics. Soil Sci. Soc. Am. J. **48**, 769 (1984) doi:10.2136/sssaj1984.03615995004800040014x.
25. Sparks, D. L.: New Frontiers in Elucidating the Kinetics and Mechanisms of Metal and Oxyanion Sorption at the Soil Mineral/water Interface. J. Plant Nutr. Soil Sci. **163**, 563–570 (2000) doi:10.1002/1522-2624(200012)163:6<563::AID-JPLN563>3.0.CO;2-0.
26. Sparks, D. L.: Kinetics of Soil Chemical Phenomena: Future Directions. In: *Future Prospects for Soil Chemistry*. SSSA Special Publication. Soil Science Society of America, Madison, WI (1998) pp. 81–101.
27. Schwertmann, U.: The Influence of Aluminum on Iron Oxides: IX. Dissolution of Al-Goethites in 6 M HCl. Clay Miner. **19**, 9–19 (1984) doi:10.1180/claymin.1984.019.1.02.
28. Fischer, L.; Muhlen, E. Z.; Brummer, G. W.; Niehus, H.: Atomic Force Microscopy (AFM) Investigations of the Surface Topography of a Multidomain Porous Goethite. Eur. J. Soil Sci. **47**, 329–334 (1996) doi:10.1111/j.1365-2389.1996.tb01406.x.
29. Bruemmer, G. W.; Gerth, J.; Tiller, K. G.: Reaction Kinetics of the Adsorption and Desorption of Nickel, Zinc and Cadmium by Goethite. I. Adsorption and Diffusion of Metals. J. Soil Sci. **39**, 37–52 (1988) doi:10.1111/j.1365-2389.1988.tb01192.x.
30. Eick, M. J.; Peak, J. D.; Brady, P. V.; Pesek, J. D.: Kinetics of Lead Adsorption/Desorption on Goethite: Residence Time Effect. Soil Sci. **164**, 28–39 (1999) doi:10.1097/00010694-199901000-00005.
31. Kim, C. S.; Lentini, C. J.; Waychunas, G. A.: Associations between Iron Oxyhydroxide Nanoparticle Growth and Metal Adsorption/Structural Incorporation. In: *Adsorption of Metals by Geomedia II: Variables, Mechanisms, and Model Applications*. (Bernett, M. O., Kent, D., Eds.) Developments in Earth and Environmental Sciences. Vol. 7, Elsevier (2007) pp. 153–185.
32. Sparks, D. L.: Kinetics and Mechanisms of Chemical Reactions at the Soil Mineral/Water Interface. In: *Soil Physical Chemistry*. CRC Press, Boca Raton, FL (1998) pp. 135–191.
33. Barrow, N. J.; Brümmer, G. W.; Fischer, L.: Rate of Desorption of Eight Heavy Metals from Goethite and Its Implications for Understanding the Pathways for Penetration. Eur. J. Soil Sci. **63**, 389–398 (2012) doi:10.1111/j.1365-2389.2012.01450.x.
34. Ainsworth, C. C.; Gassman, P. L.; Pilon, J. L.; Sluys, V. D.; G, W.: Cobalt, Cadmium, and Lead Sorption to Hydrous Iron Oxide: Residence Time Effect. Soil Sci. Soc. Am. J. **58**, 1615–1623 (1994) doi:10.2136/sssaj1994.03615995005800060005x.
35. Sanchez, A. L.; Murray, J. W.; Sibley, T. H.: The Adsorption of Plutonium IV and V on Goethite. Geochim. Cosmochim.

Ac. **49**, 2297–2307 (1985) doi:10.1016/0016-7037(85)90230-3.
36. Keeney-Kennicutt, W. L.; Morse, J. W.: The Redox Chemistry of $Pu(V)O_2^+$ Interaction with Common Mineral Surfaces in Dilute Solutions and Seawater. Geochim. Cosmochim. Ac. **49**, 2577–2588 (1985) doi:10.1016/0016-7037(85)90127-9.
37. Penrose, W. R.; Metta, D. N.; Hylko, J. M.; Rinckel, L. A.: The Reduction of Plutonium(V) by Aquatic Sediments. J. Environ. Radioact. **5**, 169–184 (1987) doi:10.1016/0265-931X(87)90033-6.
38. Powell, B. A.; Fjeld, R. A.; Kaplan, D. I.; Coates, J. T.; Serkiz, S. M.: $Pu(V)O_2^+$ Adsorption and Reduction by Synthetic Hematite and Goethite. Environ. Sci. Technol. **39**, 2107–2114 (2005) doi:10.1021/es0487168.
39. Powell, B. A.; Fjeld, R. A.; Kaplan, D. I.; Coates, J. T.; Serkiz, S. M.: $Pu(V)O_2^+$ Adsorption and Reduction by Synthetic Magnetite (Fe_3O_4). Environ. Sci. Technol. **38**, 6016–6024 (2004) doi:10.1021/es049386u.
40. Romanchuk, A. Y.; Kalmykov, S. N.; Aliev, R. A.: Plutonium Sorption onto Hematite Colloids at Femto- and Nanomolar Concentrations. Radiochim. Acta **99**, 137–144 (2011) doi:10.1524/ract.2011.1808.
41. Choppin, G.; Bond, A.; Hromadka, P.: Redox Speciation of Plutonium. J. Radioanal. Nucl. Chem. **219**, 203–210 (1997) doi:10.1007/BF02038501.
42. Silva, R. J.; Nitsche, H.: Actinide Environmental Chemistry. Radiochim. Acta **70/71**, 377–396 (1995).
43. Cleveland, J.: *The Chemistry of Plutonium*. American Nuclear Society, La Grange Park, IL (1979).
44. Morse, J. W.; Choppin, G. R.: Laboratory Studies of Plutonium in Marine Systems. Mar. Chem. **20**, 73–89 (1986) doi:10.1016/0304-4203(86)90067-8.
45. Orlandini, K. A.; Penrose, W. R.; Nelson, D. M.: Pu(V) as the Stable Form of Oxidized Plutonium in Natural Waters. Mar. Chem. **18**, 49–57 (1986) doi:10.1016/0304-4203(86)90075-7.
46. Rai, D.: Solubility Product of Pu(IV) Hydrous Oxide and Equilibrium Constants of Pu(IV)/Pu(V), Pu(IV)/Pu(VI), and Pu(V)/Pu(VI) Couples. Radiochim. Acta **35**, 97–106 (1984).
47. Rai, D.; Sern, R. J.; Swanson, J. L.: Solution Species of Plutonium in the Environment. J. Environ. Qual. **9**, 417–420 (1980).
48. Rai, D.; Moore, D. A.; Felmy, A. R.; Choppin, G. R.; Moore, R. C.: Thermodynamics of the $PuO_2^+ – Na^+ – OH^- – Cl^- – ClO_4^- – H_2O$ System: Use of NpO_2^+ Pitzer Parameters for PuO_2^+. Radiochim. Acta **89**, (2001) doi:10.1524/ract.2001.89.8.491.
49. Banik, N. L.; Buda, R. A.; Bürger, S.; Kratz, J. V.; Trautmann, N.: Sorption of Tetravalent Plutonium and Humic Substances onto Kaolinite. Radiochim. Acta **95**, 569–575 (2007) doi:10.1524/ract.2007.95.10.569.
50. Buda, R.; Banik, N. L.; Kratz, J. V.; Trautmann, N.: Studies of the Ternary Systems Humic Substances – Kaolinite – Pu(III) and Pu(IV). Radiochim. Acta **96**, (2008) doi:10.1524/ract.2008.1550.
51. Powell, B. A.; Duff, M. C.; Kaplan, D. I.; Fjeld, R. A.; Neville, M.; Hunter, D. B.; Bertsch, P. M.; Coates, J. T.; Eng, P.; Rivers, M. L.; *et al.*: Plutonium Oxidation and Subsequent Reduction by Mn(IV) Minerals in Yucca Mountain Tuff. Environ. Sci. Technol. **40**, 3508–3514 (2006) doi:10.1021/es052353+.
52. Guillaumont, R.; Fanghanel, T.; Fuger, J.; Grenthe, I.; Neck, V.; Palmer, D. A.; Rand, M. H.: *Update on the Chemical Thermodynamics of Uranium, Neptunium, Plutoniuim, Americium and Technicium*. Mompean, F. J., Illemassene, M., Domenech-Orti, C., Said, K. Ben, Eds. Chemical

Thermodynamics Series, Vol. 5, North Holland ElsevierScience B. V., Amsterdam (2003).
53. Powell, B. A.; Kersting, A.; Zavarin, M.; Zhao, P.: Development of a Composite Non-Electrostatic Surface Complexation Model Describing Plutonium Sorption to Aluminosilicates. Lawrence Livermore National Laboratory, Livermore, CA. LLNL-TR-408276 (2011).
54. Boukhalfa, H.; Reilly, S. D.; Neu, M. P.: Complexation of Pu(IV) with the Natural Siderophore Desferrioxamine B and the Redox Properties of Pu(IV)(siderophore) Complexes. Inorg. Chem. **46**, 1018–1026 (2007) doi:10.1021/ic061544q.
55. Keberle, H.: The Biochemistry of Desferrioxamine and Its Relation to Iron Metabolism. Ann. NY Acad. Sci. **119**, 758–768 (1964) doi:10.1111/j.1749-6632.1965.tb54077.x.
56. Foti, S. C.; Freiling, E. C.: The Determination of the Oxidation States of Tracer Uranium, Neptunium and Plutonium in Aqueous Media. Talanta **11**, 385–392 (1964) doi:10.1016/0039-9140(64)80047-3.
57. Nitsche, H.; Lee, S. C.; Gatti, R. C.: Determination of Plutonium Oxidation States at Trace Levels Pertinent to Nuclear Waste Disposal. J. Radioanal. Nucl. Chem. **124**, 171–185 (1988).
58. Neu, M.; Hoffman, D.; Roberts, K.; Nitsche, H.; Silva, R. J.: Comparison of Chemical Extractions and Laser Photoacoustic-Spectroscopy for the Determination of Plutonium Species in Near-Neutral Carbonate Solutions. Radiochim. Acta **66**, 251–258 (1994).
59. Cheah, S.-F.; Kraemer, S. M.; Cervini-Silva, J.; Sposito, G.: Steady-State Dissolution Kinetics of Goethite in the Presence of Desferrioxamine B and Oxalate Ligands: Implications for the Microbial Acquisition of Iron. Chem. Geol. **198**, 63–75 (2003) doi:10.1016/S0009-2541(02)00421-7.
60. Kraemer, S. M.; Cheah, S.-F.; Zapf, R.; Xu, J.; Raymond, K. N.; Sposito, G.: Effect of Hydroxamate Siderophores on Fe Release and Pb(II) Adsorption by Goethite. Geochim. Cosmochim. Ac. **63**, 3003–3008 (1999) doi:10.1016/S0016-7037(99)00227-6.
61. Cocozza, C.; Tsao, C. C. G.; Cheah, S.-F.; Kraemer, S. M.; Raymond, K. N.; Miano, T. M.; Sposito, G.: Temperature Dependence of Goethite Dissolution Promoted by Trihydroxamate Siderophores. Geochim. Cosmochim. Ac. **66**, 431–438 (2002) doi:10.1016/S0016-7037(01)00780-3.
62. Wateau, F.; Berthelin, J.: Microbial Dissolution of Iron and Aluminum from Soil Minerals: Efficiency and Specificity of Hydroxamate Siderophores Compared to Aliphatic Acids. Eur. J. Soil Biol. **30**, 1–9 (1994).

Effect of Equilibration Time on Pu Desorption from Goethite

Jennifer C. Wong,*,† Mavrik Zavarin,‡ James D. C. Begg,‡ Annie B. Kersting,‡ Brian A. Powell*,†

†Department of Environmental Engineering and Earth Sciences, Clemson University, 342 Computer Court, Anderson, South Carolina 29625, USA

‡Glenn T. Seaborg Institute, Lawrence Livermore National Laboratory, 7000 East Avenue, Livermore, California 94551, USA

*Corresponding authors: Brian A. Powell, 342 Computer Court, Anderson, SC 29625, USA, bpowell@clemson.edu; Jennifer C. Wong, jwong@clemson.edu.

Submitted: February XX, 2015

This document consists of 11 pages. It includes 6 figures, 3 tables, and 2 equations.

Contents

Pu Speciation in the Presence of DFOB (Fig. A1)

In the presence of DFOB, Pu(IV) species in the form of $PuDFOB^{2+}$, $PuH_2(DFOB)_2^{2+}$, and $Pu(OH)_{4(aq)}$ dominate a large range of pH and E_h conditions.

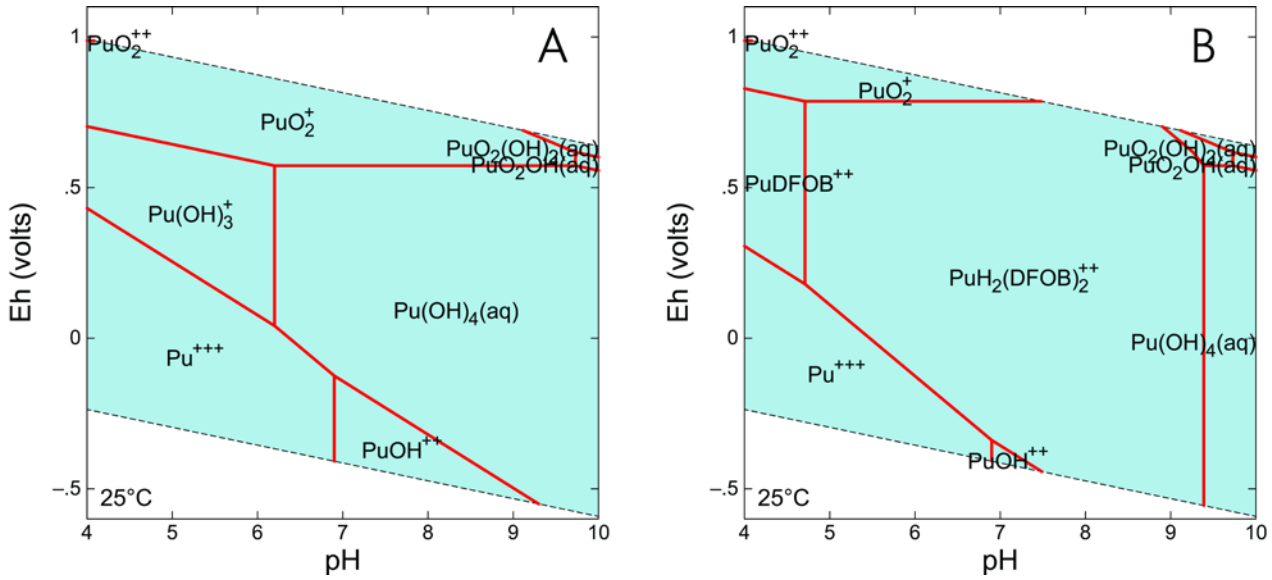

Fig. A1. Equilibrium speciation for 10^{-10} M Pu (A) in the absence of DFOB and (B) in the presence of 1.7 µM DFOB. PuO_2 minerals suppressed and 10 mM NaCl is included. Constants are from refs [1, 2]. (Geochemist's Workbench Standard 8.0).

Pu Speciation in the Presence of DFOB and Fe(III) (Fig. A2)

In the presence of 1.7 µM DFOB and 1.0 µM Fe^{3+}, Pu(IV)–DFOB species in the form of $PuDFOB^{2+}$ and $PuH_2(DFOB)_2^{2+}$ dominate over $Pu(OH)_x^{4-x}$ species at experimentally relevant pH values.

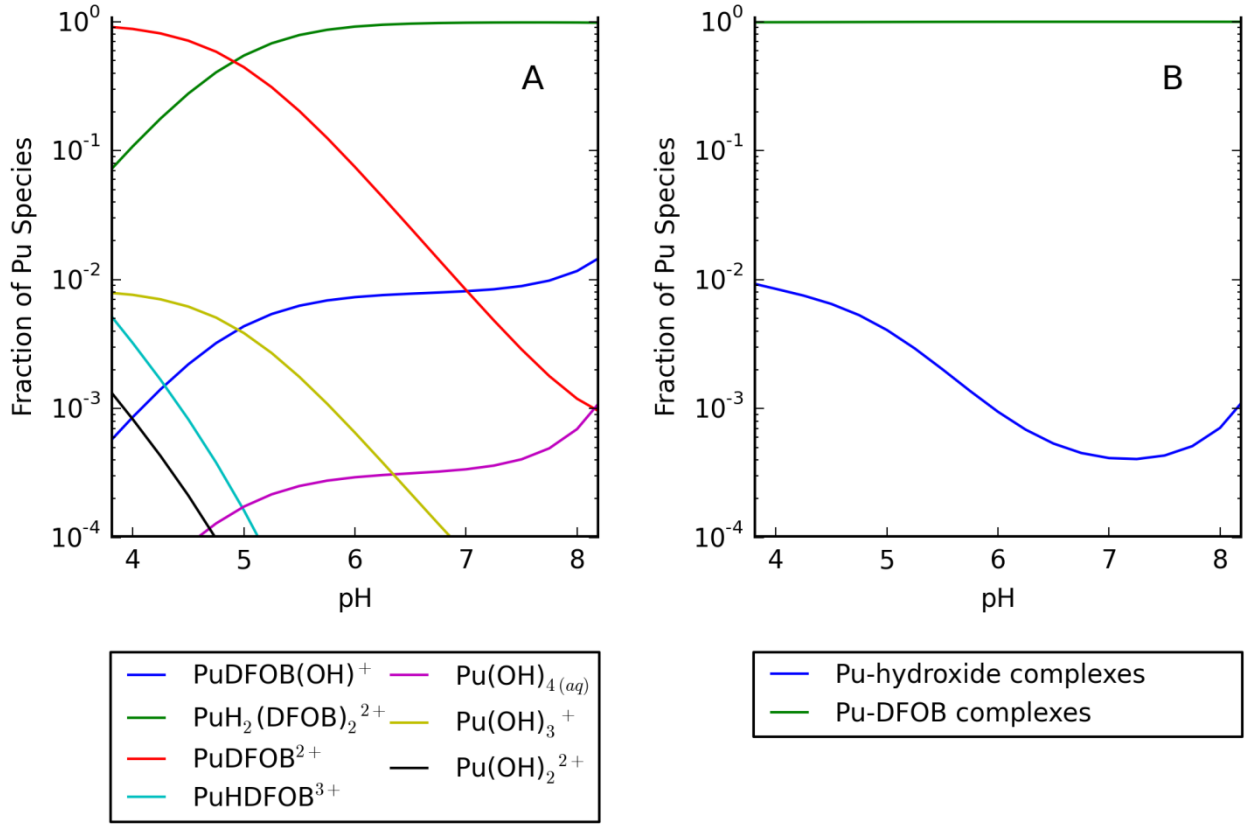

Fig. A2. (A) Equilibrium speciation of 10^{-10} M Pu(IV) in the presence of 1.7 µM DFOB, 1.0 µM Fe^{3+} and 10 mM NaCl. (B) Total fractions $Pu(OH)_x^{4-x}$ and Pu(IV)–DFOB species are shown. Constants are from refs [1–3].

Isotherms for DFOB Sorption to Goethite (Fig. A3)

The DFOB surface coverage was estimated by using published sorption isotherms [4, 5] to extrapolate to 1.7 µM total DFOB and 0.10 g/L goethite. Based on the Langmuir isotherm model (Eq. 1) shown in Fig. A3, a conservative estimate for the amount of DFOB sorbed to goethite is 1.1 µmol/g or 6.2%. The Langmuir isotherm model indicated a maximum surface excess, n_{max}, of 1.2 ± 0.2 µmol/g and Langmuir parameter, K_L, of 3.7 ± 2.1 µM. From linear isotherm fits to the lowest concentration measurements from Kraemer et al. (1999) and Cheah et al. (2003), the amount of DFOB sorbed to goethite is 0.7 µmol/g and 0.3 µmol/g or 4% and 2%, respectively.

Langmuir Equation:

$$n_{DFOB} = n_{max}\frac{K_L C}{K_L C + 1} \quad (1)$$

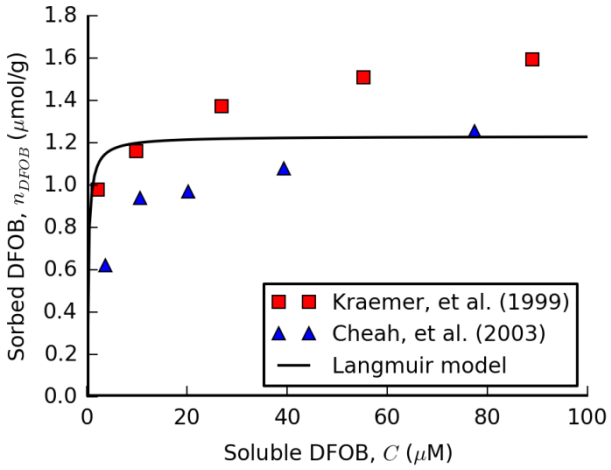

Fig. A3. The isotherm from Kraemer et al. (1999) is measured at pH 6.6 for 13 g/L goethite, 10 mM $NaClO_4$, and 5 mM MOPS buffer. The isotherm from Cheah et al. (2003) is measured at pH 5 for 10 g/L goethite, 10 mM $NaClO_4$, and 5 mM MOPS buffer. The Langmuir model is from Cheah et al. (2003).

Estimated Dissolved Iron in the Presence of DFOB

The iron dissolution rate was previously measured[5] at pH 6.5, in the presence of 0.5 g/L goethite, 240 µM DFOB, 5mM MOPS buffer, and 10 mM $NaClO_4$. The surface area of the goethite used by Kraemer et al. (1999) was 35 ± 3 m^2/g as determined by the static BET method.

$$0.02\,\frac{\mu mol}{g \cdot h} \times 0.1\,\frac{g}{L}(\text{goethite}) \times 24\,\frac{h}{day} \times 25\ \text{days} = 1.2\ \mu\text{mol/L} \qquad (2)$$

Batch Adsorption–Desorption Experiment in the Presence and Absence of DFOB (Fig. A4, Tables A1–A3)

Solutions of 10 mM NaCl and 0.075 g/L synthetic goethite were prepared in 15 mL polyethylene tubes. After addition of Pu from Pu(IV) or Pu–DFOB stock solutions, the final Pu concentration of samples was 1.7×10^{-10} M for DFOB-containing samples and 1.9×10^{-10} M for DFOB-free samples. Additional DFOB was added to DFOB-containing samples from the DFOB stock solution to yield 1.7 μM DFOB. Samples were adjusted to pH 6 and 8 with dilute HCl and NaOH. After 25 days' adsorption, experiments were phase separated and supernatants exchanged for fresh Pu-free solutions of the same pH and DFOB concentration. During desorption, aqueous Pu was measured at 3 hours, 5 hours, 18 hours, 3 days, and 12 days.

Table A1. Percent Pu sorbed during adsorption step

DFOB Conc. (μM)	pH	2 hours	5 hours	1 day	3 days	10 days	25 days
0.0	6	84.9 ± 0.4	82.1 ± 0.4	71.8 ± 0.5	70.2 ± 0.5	79.8 ± 0.4	83.3 ± 0.4
0.0	8	87.74 ± 0.3	87.28 ± 0.3	89.42 ± 0.3	92.8 ± 0.3	96.04 ± 0.20	98.40 ± 0.14
1.7	6	9.7 ± 1.0	10.1 ± 1.0	21.7 ± 0.9	8.7 ± 1.0	23.3 ± 0.9	27.7 ± 1.5
1.7	8	22.6 ± 0.9	30.6 ± 0.8	24.3 ± 0.9	26.8 ± 0.9	38.5 ±0.8	43.9 ± 1.2

Table A2. Estimated First Order Adsorption Rate Constants (s^{-1}).

pH	DFOB-free	1.7 μM DFOB
6	$9 \pm 16 \times 10^{-8}$	$9 \pm 4 \times 10^{-8}$
8	$9.4 \pm 0.9 \times 10^{-7}$	$1.4 \pm 0.8 \times 10^{-7}$

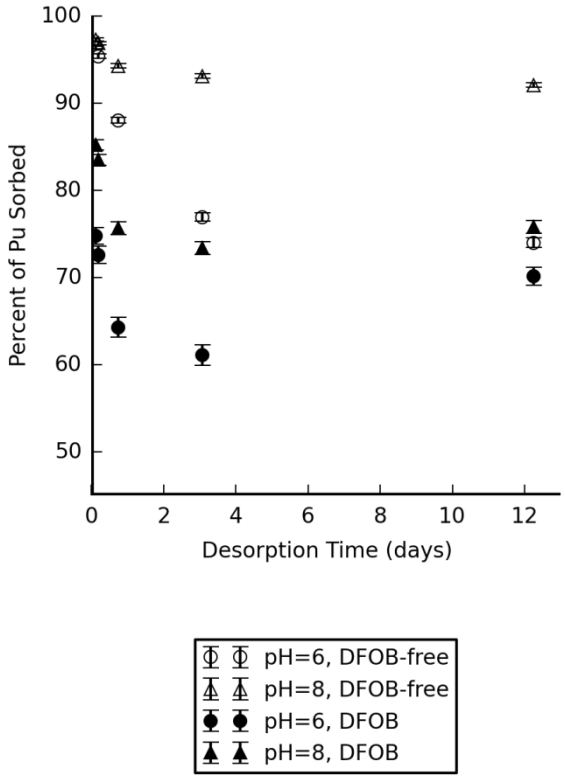

Fig. A4. The percent of Pu sorbed is plotted against time for Pu desorption from 0.075 g/L goethite suspensions with 10 mM NaCl for ionic strength control. Pu was initially added as Pu(IV) to samples containing 1.7 μM DFOB and DFOB-free solutions. Error bars represent two standard deviations of measurement uncertainty derived from counting statistics. The first data point was collected after a 3 hour desorption time period.

Table A3. Percent Pu sorbed during desorption step

DFOB Conc. (μM)	pH	3 hours	5 hours	18 hours	3 days	12 days
0.0	6	96.44 ± 0.22	95.41 ± 0.24	88.1 ±0.4	76.9 ± 0.5	74.0 ± 0.5
0.0	8	97.32 ± 0.17	96.90 ± 0.18	94.30 ± 0.24	93.13 ±0.25	92.1 ±0.3
1.7	6	74.8 ± 1.0	72.6 ± 1.0	64.3 ± 1.1	61.1 ± 1.2	70.2 ± 1.0
1.7	8	85.2 ± 0.6	83.5 ± 0.6	75.7 ± 0.7	73.4 ± 0.8	75.8 ± 0.7

Batch Experiments with Varying Adsorption Equilibration Time: Adsorption Measurements (Fig. A5)

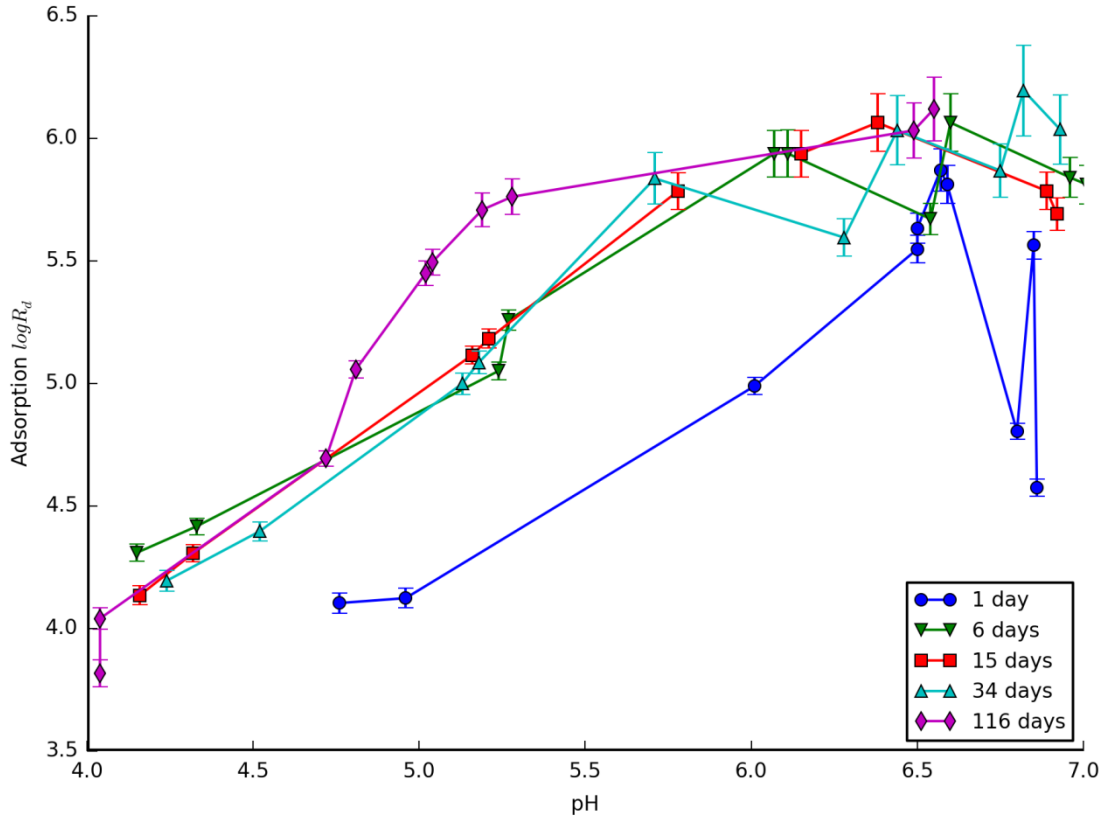

Fig. A5. Logarithmic adsorption distribution ratios (R_d) for Pu on 0.10 g/L goethite suspensions as a function of pH and time. Total Pu concentration is 1.2×10^{-10} M, and ionic strength was controlled with 10 mM NaCl. Error bars indicate two standard deviations of measurement uncertainty derived from counting statistics.

HR-TEM Images of Goethite Micropores (Fig. A6)

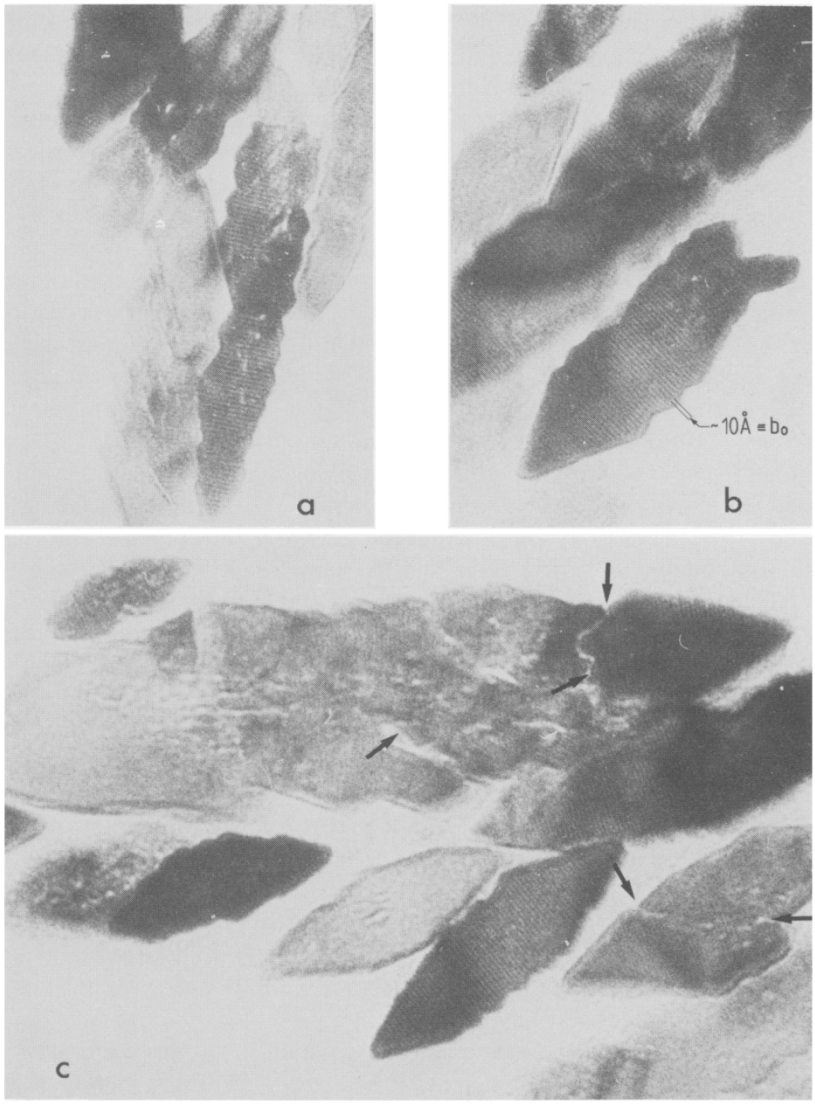

Fig. A6. A high resolution tunneling electron microscope image of a thin section showing goethite laths cut perpendicular to the c-axis. Arrows indicate micropores occurring at the boundaries of crystallite domains. Republished with permission of the Mineralogical Society (Great Britain), from Schwertmann, U.: The Influence of Aluminum on Iron Oxides: IX. Dissolution of Al-Goethites in 6 M HCl. Clay Minerals **19**, 9–19 (1984).

References

1. Boukhalfa, H.; Reilly, S. D.; Neu, M. P.: Complexation of Pu(IV) with the Natural Siderophore Desferrioxamine B and the Redox Properties of Pu(IV)(siderophore) Complexes. Inorg. Chem. **46**, 1018–1026 (2007) doi:10.1021/ic061544q.
2. Guillaumont, R.; Fanghanel, T.; Fuger, J.; Grenthe, I.; Neck, V.; Palmer, D. A.; Rand, M. H.: *Update on the Chemical Thermodynamics of Uranium, Neptunium, Plutoniuim, Americium and Technicium*. Mompean, F. J., Illemassene, M., Domenech-Orti, C., Said, K. Ben, Eds. Chemical Thermodynamics Series, Vol. 5, North Holland ElsevierScience B. V., Amsterdam (2003).
3. Kraemer, S. M.: Iron Oxide Dissolution and Solubility in the Presence of Siderophores. Aquat. Sci. **66**, 3–18 (2004) doi:10.1007/s00027-003-0690-5.
4. Cheah, S.-F.; Kraemer, S. M.; Cervini-Silva, J.; Sposito, G.: Steady-State Dissolution Kinetics of Goethite in the Presence of Desferrioxamine B and Oxalate Ligands: Implications for the Microbial Acquisition of Iron. Chem. Geol. **198**, 63–75 (2003) doi:10.1016/S0009-2541(02)00421-7.
5. Kraemer, S. M.; Cheah, S.-F.; Zapf, R.; Xu, J.; Raymond, K. N.; Sposito, G.: Effect of Hydroxamate Siderophores on Fe Release and Pb(II) Adsorption by Goethite. Geochim. Cosmochim. Ac. **63**, 3003–3008 (1999) doi:10.1016/S0016-7037(99)00227-6.
6. Schwertmann, U.: The Influence of Aluminum on Iron Oxides: IX. Dissolution of Al-Goethites in 6 M HCl. Clay Miner. **19**, 9–19 (1984) doi:10.1180/claymin.1984.019.1.02.